Extrasolar Cosmochemistry

M. Jura[1] and E.D. Young[2]

[1]Department of Physics and Astronomy and [2]Department of Earth and Space Sciences, University of California, Los Angeles, California 90095; email: jura@astro.ucla.edu, eyoung@ess.ucla.edu

Annu. Rev. Earth Planet. Sci. 2014. 42:45–67

The *Annual Review of Earth and Planetary Sciences* is online at earth.annualreviews.org

This article's doi:
10.1146/annurev-earth-060313-054740

Keywords

planetary systems, white dwarfs

Abstract

Evidence is now compelling that elements heavier than helium in many white dwarf atmospheres have accumulated by accretion from orbiting rocky bodies, often larger than 100 km in diameter, such as asteroids. Consequently, we now possess a powerful tool to measure the elemental constituents of extrasolar minor planets. To zeroth order, the accreted extrasolar parent bodies resemble bulk Earth: They are at least 85% by mass composed of oxygen, magnesium, silicon, and iron; carbon and ice are only trace constituents. Assembled data for white dwarf pollutions suggest that differentiation of extrasolar planetesimals, leading to iron-rich cores and aluminum-rich crusts, is common. Except for instances of unexpectedly high calcium abundances, the compositions of extrasolar planetesimals can be understood as resulting from processes similar to those controlling the formation and evolution of objects in the inner Solar System.

1. INTRODUCTION

What are the elemental compositions of extrasolar planets and planetesimals? Are they familiar or exotic? Which, if any, extrasolar planetesimals experience differentiation? Externally polluted white dwarfs provide an opportunity to address these questions.

After undergoing extensive evolution, stars with initial main-sequence masses less than eight times that of the Sun ultimately shed most of their primordial material and shrink in size to become white dwarfs composed primarily of carbon and oxygen. Such white dwarfs typically retain a thin outer envelope of hydrogen and/or helium, the dominant constituent in the observable atmosphere. These stars are typically the radius of Earth and slowly cool from an initial outer temperature above 100,000 K. Once the effective temperature of the atmosphere falls below 20,000 K, radiative levitation—the process of supporting an element in the atmosphere by the upward flow of radiation—becomes unimportant (Chayer et al. 1995). During this relatively cool phase, gravitational settling is sufficiently rapid that all elements heavier than helium sink into the undetectable interior in a time much shorter than the white dwarf's cooling age. Consequently, most of these cooler white dwarfs display very simple spectra and show lines of only hydrogen or, more rarely, only helium.

There are exceptions. Between 1/4 and 1/3 of all white dwarfs cooler than 20,000 K display the presence of heavy atoms in their atmospheres (Zuckerman et al. 2003, 2010). Until ten years ago, it was usually thought that the accreted matter originates in the interstellar medium (Dupuis et al. 1992, 1993; Hansen & Liebert 2003), although comets or minor planets also were suggested as sources of the material (Alcock et al. 1986, Aannestad et al. 1993). During the past decade, amassed evidence has provided compelling support for the scenario that the heavy elements derive from rocky planetesimals (Jura 2008, 2014). The widely accepted model is that an asteroid's orbit is perturbed so that it passes within the white dwarf's tidal radius, where it is destroyed, a circumstellar disk is formed, and eventually this material is accreted onto the host star (Debes & Sigurdsson 2002, Jura 2003). Consequently, spectroscopic determination of the abundances in externally polluted white dwarfs is an indirect but uniquely powerful tool to measure the detailed elemental compositions of accreted extrasolar minor planets.

In Section 2, we describe how to translate observations of relative abundances in the atmosphere of a white dwarf into relative abundances in the accreted parent body. In Section 3, we review estimates of the masses of individual parent bodies and of the total mass of the ensemble of minor planets required to produce the observed depletions. In Section 4, we give an overview of existing data. In Section 5, we describe results that most likely are the consequence of planetesimal formation in protoplanetary disks. Then, in Section 6, we describe results that pertain to the evolution of planetesimals beyond their phase of nebular formation. Finally, in Section 7, we present our conclusions and suggest directions of future research.

2. MODELING THE ACCRETION EVENTS

The pollution of a white dwarf is a three-step process. First, an asteroid has its orbit perturbed so that it passes within the tidal radius of its host white dwarf. Second, an asteroid is tidally disrupted and a disk forms. Third, there is accretion from the disk onto the star. **Figure 1** provides a schematic picture.

2.1. Asteroid Survival and Subsequent Orbital Perturbations

During its evolution as a red giant before it becomes a white dwarf, a star loses much of its initial main-sequence mass. For example, a star that is initially 2.0 $M_{\odot}$ on the main sequence is thought

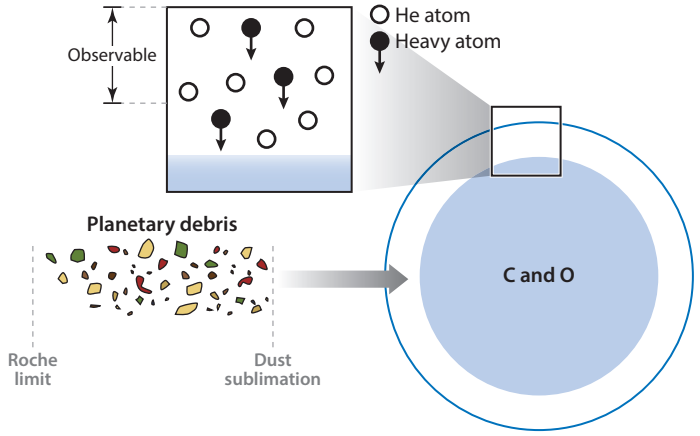

Figure 1

Schematic picture of an accreting white dwarf.

to become a white dwarf with a mass of 0.60 $M_\odot$ (Williams et al. 2009). However, this mass loss is relatively slow in the sense that it takes much longer than an asteroid's orbital period. As a consequence, the asteroid's angular momentum is approximately conserved, and it migrates outward but is still gravitationally bound (Duncan & Lissauer 1998). If initially further than 2.5 AU (AU = astronomical unit = 1.5×10^{13} cm) from the star while on the main sequence, asteroids should survive both intense heating from the red giant and frictional drag from the ejected stellar matter if they are greater than 10 km in radius (Jura 2008). Although there are uncertainties, dynamical models describe how some of these surviving planetesimals subsequently have their orbits perturbed by a surviving planet into the white dwarfs' tidal zone (Debes & Sigurdsson 2002; Bonsor et al. 2011; Veras et al. 2011, 2013; Debes et al. 2012b).

2.2. Disk Formation and Evolution

White dwarfs typically have mean densities more than 10^5 times greater than the Sun's. Therefore, even though the white dwarf has a radius of only 0.01 $R_\odot$, where $R_\odot$ denotes the radius of the Sun, i.e., 7.0×10^{10} cm, it can tidally disrupt an asteroid of mean density 3 g cm^{-3} out to an approximate distance of 1 $R_\odot$ (Davidsson 1999). Although the process is not yet modeled in detail, we expect that the fragments of the disruption will undergo mutual collisions in which energy but not angular momentum is lost (Jura 2003, Debes et al. 2012b). Consequently, a disk is formed.

Dust disks can be identified orbiting white dwarfs because they absorb the optical and UV light emitted by the star and re-emit in the infrared, thereby producing excess radiation at these longer wavelengths (Zuckerman & Becklin 1987; Becklin et al. 2005; Kilic et al. 2005, 2006; Reach et al. 2005; Jura et al. 2007; Farihi et al. 2009; Debes et al. 2012a; Xu & Jura 2012). Circumstellar gas associated with the dust is also sometimes detected from characteristic double-peaked emission (Gaensicke et al. 2006, 2007, 2008; Melis et al. 2010, 2012; Farihi et al. 2012a) or, more rarely, from absorption (Debes et al. 2012b, Gaensicke et al. 2012). Dust disks are almost exclusively detected around stars hotter than 10,000 K (Xu & Jura 2012), even though many cooler white dwarfs are known to accrete. Estimates of the fraction of white dwarfs warmer than 10,000 K with dust disks range from 1% to 3% (Farihi et al. 2009) to 4% (Barber et al. 2012). There is a strong correlation between being highly polluted and having a dust disk, but only approximately 1/5 to 1/10 of all polluted white dwarfs possess circumstellar dust.

For the disks with dust, the Poynting–Robertson effect, the process by which light from the central star is absorbed and then re-emitted by orbiting material, which itself then loses angular moment and spirals inward, must operate and produce a lower bound to the rate of accretion (Rafikov 2011a). However, there are stars for which the accretion rate is appreciably greater than that predicted by this process, and viscosity in associated gas likely is important (Rafikov 2011b, Metzger et al. 2012). In stars without dust, viscosity in the gaseous disk likely drives the infall (Jura 2008). The lifetimes of the dust disks are highly uncertain; 0.4 Myr is estimated to be typical but with a factor of 10 uncertainty (Girven et al. 2012).

2.3. Photospheric Signatures of Accretion

Using standard stellar model atmosphere theory and the observed spectra, we determine photospheric abundances of the different heavy elements in the atmosphere of an externally polluted white dwarf. However, the abundances in the photosphere do not necessarily directly translate into the abundances in the accreted parent body (PB). Much depends upon whether there is a convective zone and, if so, its size. The usual criterion for the onset of convection is determined by the opacity, composition, and temperature of the gas. Stars with helium-dominated atmospheres have convective zones with masses as much as 10^{-5} of that of the star. In contrast, the atmospheres of white dwarfs with hydrogen-dominated atmospheres have small or no convective zones. The mass of the outer region, where we consider the mixing of heavy elements with H, can be less than 10^{-16} the mass of the star. Therefore, the correction for how to scale between the photospheric abundances and the composition of the parent body strongly depends upon the dominant element in the star's atmosphere.

The mass of the Zth element in the outer mixing zone of a white dwarf, $M_*(Z)$, is governed by considering the rate of mass gain from accretion, $\dot{M}_{\rm PB}(Z)$, and the rate of mass loss described by settling with the expression (Koester 2009)

$$\frac{{\rm d}M_*(Z)}{{\rm d}t} = -\frac{M_*(Z)}{t_Z} + \dot{M}_{\rm PB}(Z), \tag{1}$$

where t_Z denotes the Zth element's settling time. Assuming that $M_*(Z) = 0$ at $t = 0$, the solution to Equation 1 is

$$M_*(Z) = e^{-t/t_Z} \int_0^t e^{t'/t_Z} \dot{M}_{\rm PB}(Z){\rm d}t'. \tag{2}$$

We measure $M_*(Z)$ in the star's outer mixing zone; we aim to determine $\dot{M}_{\rm PB}(Z)$.

If the star has a convective zone, then t_Z is defined by the time for an element to diffuse out of the zone into a lower stable layer. If the star does not have a convective zone, then t_Z is defined by the time to diffuse below the thin outer atmosphere that is studied spectroscopically. There are orders of magnitude differences between the two timescales.

As described by Koester (2009), there are important limiting case solutions to Equation 2. If the accretion rate is nearly constant and if $t \ll t_Z$, the system is in a buildup phase and the atmospheric abundance is directly given by the accretion rate; the approximate solution to Equation 2 is

$$M_*(Z) \approx \dot{M}_{\rm PB}(Z)t. \tag{3}$$

If so, then for any two elements denoted by j and k, the ratio between the masses of detectable material is

$$\frac{\dot{M}_{\rm PB}(Z_j)}{\dot{M}_{\rm PB}(Z_k)} = \frac{M_*(Z_j)}{M_*(Z_k)}. \tag{4}$$

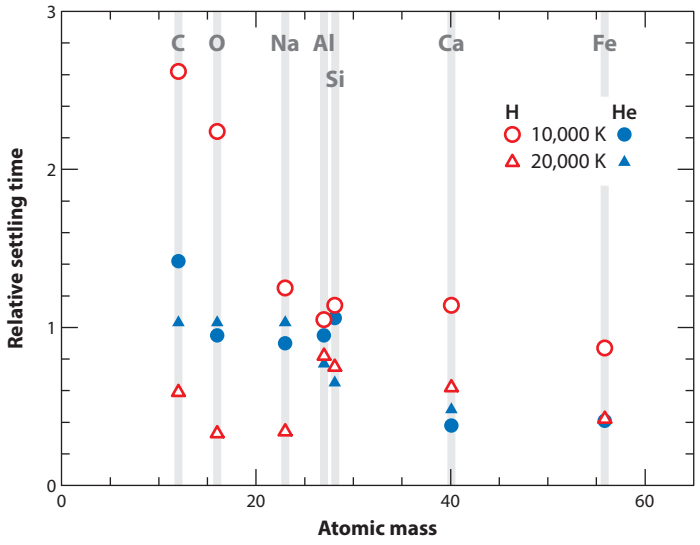

Figure 2

Settling times on a linear scale relative to magnesium's. The red open and blue filled points are for white dwarfs with H-dominated and He-dominated atmospheres, respectively. Circles and triangles are for atmospheres of 10,000 K and 20,000 K, respectively. The gravitational acceleration is always assumed to equal 10^8 cm s^{-2}. The calculations are described by Koester (2009), and updated values are provided by Koester (2013).

That is, the relative abundance in the photosphere directly reflects the abundance in the parent body.

A second phase may be a steady state that prevails when $t > t_Z$ for all elements of interest yet accretion continues. In this case, if $\dot{M}_{\rm PB}(Z)$ is constant, the approximate solution to Equation 2 is that

$$M_*(Z) \approx \dot{M}_{\rm PB}(Z) t_Z. \tag{5}$$

If so, then for any two elements denoted by j and k, the ratio between the masses of detectable material is

$$\frac{\dot{M}_{\rm PB}(Z_j)}{\dot{M}_{\rm PB}(Z_k)} = \frac{M_*(Z_j)}{M_*(Z_k)} \frac{t_{Z,k}}{t_{Z,j}}. \tag{6}$$

In this case, to determine the abundances in the parent body, it is necessary to compute the relative settling times in addition to measuring the relative photospheric abundances.

We see by comparing Equations 4 and 6 that the difference in the abundance ratios between the instantaneous and steady-state models depends upon the ratio of the settling times. Although settling times are sensitive to the star's effective temperature and gravity, relative to magnesium's settling time, as illustrated in **Figure 2**, the settling of a lighter element such as C may be a factor of 2 slower, whereas a heavier element such as Fe may be a factor of 2 faster. Therefore, unless we consider elements with nearly the same settling times, uncertainties of a factor of 2 in the relative abundances may ensue if we do not know the phase of the accretion.

Besides the two cases considered above, a third phase may occur when accretion has stopped but heavy elements still linger within the outer mixing zone. In this decaying phase, there may be a strong relative depletion of those heavy elements that settle the fastest. Finally, even if a white dwarf has a circumstellar disk, the accretion need not be steady with time (Rafikov 2011b,

Metzger et al. 2012). In such cases, a more complex solution to Equation 2 in which time-varying accretion occurs can be computed (Jura & Xu 2012).

Settling times are usually computed using the formalism of Dupuis et al. (1993) and are most recently reported by Koester (2013). Results for relative settling times are displayed in **Figure 2**. In stars with hydrogen-dominated atmospheres (DA stars), the settling times with $T_* > 12{,}000$ K are less than 1 year, and a steady state likely prevails. In DA stars with $T_* < 12{,}000$ K and in stars with helium-dominated atmospheres (DB and DZ stars), the settling times can be longer than 10^6 years. In these stars, the steady-state approximation may not be especially good, and a case-by-case analysis is appropriate. Here, for the DB stars, we present relative abundances measured in the stellar atmosphere without any correction for settling.

Even if the tidally disrupted parent body is highly differentiated, we assume that the disk is compositionally homogeneous. We expect that the asteroids that are accreted approach the white dwarf on highly eccentric orbits. Consequently, as the disk forms, there is considerable radial mixing of the material (Jura 2003, Debes et al. 2012a). It is also possible that a circumstellar disk is composed of several different tidally disrupted asteroids. However, if the disk is dusty, then it is likely composed of one large parent body; otherwise, mutual collisions would likely lead to complete vaporization of the solid dust particles (Jura 2008). That is, the orbital speeds of the dust are greater than 500 km s^{-1} (Gaensicke et al. 2006). Different planetesimals would likely have distinct orbital inclinations; therefore, their particles would collide at speeds in excess of 50 km s^{-1}, and even the hardiest of materials would be vaporized.

3. MASS BUDGETS

We now consider the amount of mass required in our standard model; we argue that minor planets such as asteroids are the dominant source for the pollution of white dwarf atmospheres, although there might be instances in which tidal disruption and accretion of an entire planet the size of Mars has occurred (Jura et al. 2009). For the DB stars with relatively large outer mixing zones, the minimum mass required to explain the measured heavy element pollution can be as high as 7×10^{23} g (Dufour et al. 2012), nearly the mass of Ceres, the most massive asteroid in the Solar System. However, the mass of the required parent body is usually smaller—even GD 40, one of the most heavily polluted of nearby stars, requires a minimum parent body mass of only 4×10^{22} g, which could be carried by an asteroid of approximately 300 km in diameter (Klein et al. 2010). Because neither the mass in the disk nor the mass that has previously been accreted and settled into the interior can be measured, these numbers are lower bounds and, conceivably, could be greater.

As illustrated in Equation 5, mass accretion rates can be estimated by dividing the mass of an element in the outer mixing zone, M_*, by that element's settling time, t_Z. The highest confidently estimated mass accretion rate is 1.3×10^{11} g s^{-1} (Dufour et al. 2012). However, this value is extraordinary. More typically, heavily polluted stars have inferred accretion rates near 10^9 g s^{-1} (Farihi et al. 2012b, Gaensicke et al. 2012, Xu et al. 2013b). Because the typical estimated disk lifetime is 4×10^5 years with a factor of 10 uncertainty, a large accreted parent body may have a mass of $\sim 10^{22}$ g (Girven et al. 2012).

Although the duration of any individual accretion event is unknown, we can estimate the mass required to explain the observed pollutions by considering an ensemble of systems (Zuckerman et al. 2010). In a volume-limited sample of 57 DB white dwarfs, based on the updated settling times of Koester (2013), the average accretion rate is approximately 1.4×10^8 g s^{-1} (Jura & Xu 2012). In this sample of white dwarfs with effective temperatures between 13,000 and 28,000 K, the mean cooling age—the duration of the star's white dwarf evolutionary phase—is 230 Myr.

Therefore, the typical minimum required reservoir mass is 1×10^{24} g, somewhat less than the mass of the Solar System's asteroid belt of 4×10^{24} g (Krasinsky et al. 2002).

The progenitors of white dwarfs typically have main-sequence masses greater than 1.5 $M_\odot$, and among the DB white dwarfs, these masses are typically greater than 2 $M_\odot$ (Bergeron et al. 2011). These masses correspond to F-type and A-type main-sequence stars. It has been well established from the detection of excess infrared radiation that approximately 1/3 of main-sequence A-type stars possess substantial amounts of circumstellar dust (Su et al. 2006). Much of this dust is relatively cool at a temperature of ~100 K and may be located at the equivalent of a Kuiper Belt. More recently, it has been argued that there is warmer dust also present and that approximately 1/3 of main-sequence stars possess asteroids (Morales et al. 2011, Absil et al. 2013). Among main-sequence A-type stars, dust production rates required to produce the infrared excesses as high as 10^9 g s^{-1} are common (Chen et al. 2006), often from warm dust that could have an asteroidal origin (Morales et al. 2009). Some A-type stars possess massive asteroid belts. For example, ζ Lep, an A-type main-sequence star with an estimated main-sequence age of 300 Myr, has an asteroid belt likely 100 times more massive than the Sun's (Chen & Jura 2001). Although the numbers are quite uncertain, perhaps a few percent of a typical star's asteroid belt is accreted during its white dwarf evolutionary phase. This is an important constraint on models for the dynamical evolution of ensembles of asteroids via perturbations by planets during the white dwarf phase of the star's evolution (Debes et al. 2012b).

4. OVERVIEW OF CURRENT OBSERVATIONS

Because it arises from the ground state and has a large oscillator strength, the K line of Ca II at 3933 Åusually is the strongest photospheric indicator of heavy elements in a white dwarf optical spectrum. Especially in cool white dwarfs with atmospheres largely composed of helium, whose continuum opacity can be very low, the Ca line can be much stronger than what is observed in main-sequence stars (Sion et al. 1990). Consequently, such polluted white dwarfs are easily identified with low-resolution spectra, and the brighter ones have been recognized for decades.

The era of 10-m-class ground-based telescopes equipped with high-resolution spectrographs has enabled sensitive optical studies of white dwarf spectra. In parallel, the Cosmic Origins Spectrograph (COS) on the Hubble Space Telescope has advanced substantially the capability to perform UV spectroscopy on white dwarfs. These improved technologies have greatly expanded studies of white dwarf pollutions. Major surveys include the following:

- The SPY (Supernova Ia Progenitor Survey) project was conducted at the VLT (Very Large Telescope) in Chile, and more than 1,000 white dwarfs and pre–white dwarfs were observed. Koester et al. (2005) reported photospheric Ca in approximately 3% of these stars, a few of which were previously known to be polluted. Calcium abundances were determined for these stars by Koester & Wilken (2006) and then reanalyzed for both Ca and other heavy elements, especially Mg, by Kawka et al. (2011).
- Using the HIRES (High Resolution Echelle Spectrometer) instrument on the Keck I 10-m telescope, Zuckerman et al. (2003, 2010) have observed more than 100 DAs and DBs. Because their observations were more sensitive than those of the SPY project and because they typically observed either DA stars cooler than 10,000 K or DB stars, where even small amounts of Ca are relatively easy to detect, they found that ~25% of the stars are externally polluted. These results should be taken as the best estimate for the frequency of external pollutions.
- With the SDSS (Sloan Digital Sky Survey), the number of identified white dwarfs increased from ~2,000 in the standard catalog of McCook & Sion (1999) to more than 20,000

(Kleinman et al. 2013). Even with the relatively low-resolution spectra obtained in the SDSS, calcium lines have been detected and abundances reported for more than 100 stars (Dufour et al. 2007). Up to 6 different elements heavier than He have been identified in more than 20 especially highly polluted cool white dwarfs (Koester et al. 2011).

- The snapshot mode of COS has been used to observe in the UV near 1300 Åapproximately 100 white dwarfs with 17,000 K $< T_* <$ 25,000 K (Gaensicke et al. 2012, Koester et al. 2013). Silicon has been detected in more than half of these stars, but radiative levitation can play a role, and the frequency of recent events producing external pollution is not yet well determined for this sample.
- The FUSE (Far Ultraviolet Spectroscopic Explorer) has been used to observe in the UV at $\lambda <$ 1150 Åapproximately 100 white dwarfs, most warmer than 25,000 K. Photospheric heavy elements are often present, but disentangling the line profiles and establishing the importance of external pollution have been challenging (Dickinson et al. 2012).

Currently, external pollution has been identified in more than 200 white dwarfs. In most cases, however, only Ca is detected. Abundances of at least 2 elements—typically Mg and Ca—have been measured in approximately 60 stars; in 50 stars, both Ca and Fe have been measured (Jura & Xu 2013). Elements as rare as Sr and Sc have been detected in 1 or 2 stars (Zuckerman et al. 2007, Klein et al. 2011, Dufour et al. 2012). Altogether 19 different elements heavier than helium have been detected in at least 1 star. GD 362 (Gianninas et al. 2004) has the largest known number of pollutants: 16 individual elements heavier than helium have been detected (Zuckerman et al. 2007, Xu et al. 2013b). Measurements of at least 8 distinct elements have been published for 10 white dwarfs (Zuckerman et al. 2011; Gaensicke et al. 2012; Xu et al. 2013b, 2014).

Table 1 lists properties of the 13 best-studied externally polluted white dwarfs, and **Table 2** lists the measured abundances—uncorrected for gravitational settling. One of the stars, PG 0843+516, has an effective temperature somewhat greater than 20,000 K. Therefore, in principle, radiative levitation could be of some importance. However, at this temperature, radiative levitation is important only for silicon and can only support much less of this element than is measured. Therefore, for all the stars listed in **Tables 1** and **2**, the abundances of heavy atoms appear to be controlled by the actions of accretion and gravitational settling.

5. COMPOSITIONS OF EXTRASOLAR PLANETESIMALS: NEBULAR PROCESSING

Following Xu et al. (2013b), it is useful to interpret the compositions in terms of a two-stage scenario. In the first stage, planetesimals form from the disk; for example, the water content of a planetesimal is determined by its formation location relative to a snow line. We describe results pertaining to this stage of planetesimal formation in this section. After they are formed, planetesimals continue to evolve; we describe compositional signatures from differentiation and mutual collisions in the next section.

5.1. The Dominant Elements

The overall composition of a planetesimal may be determined by conditions in the protoplanetary nebula. In the Solar System, Earth and chondrites are more than 90% by mass composed of four elements: O, Mg, Si, and Fe. However, Bond et al. (2010) have suggested that extrasolar planetesimals may have a very different set of dominant elements. In particular, Bond et al. proposed the formation of either C-dominated planetesimals or planetesimals largely composed of very refractory elements such as Ca and Al—essentially, enormous extrasolar counterparts to

Table 1 Heavily polluted white dwarfs[1]

Number	Name	WD	Dom.	T_* (K)	Dust	[Mg]/[X]	Number of elements	Reference(s)
1	GD 40	0300-013	He	15,300	Yes	−6.20	12	Klein et al. 2010, Jura et al. 2012, Xu et al. 2013b
2	GD 61	0435+410	He	17,300	Yes	−6.69	5	Farihi et al. 2011, 2013
3		J0738+1835	He	14,000	Yes	−4.68	14	Dufour et al. 2012
4	PG 0843+516	0843+516	H	23,100	Yes	−5.00	10	Gaensicke et al. 2012
5	PG 1015+161	1015+161	H	19,200	Yes	−5.30	5	Gaensicke et al. 2012
6	PG 1225-079	1225-079	He	10,800	Yes	−7.50	11	Xu et al. 2013b, Klein et al. 2011
7		1226+110	H	20,900	Yes	−5.20	7	Gaensicke et al. 2012
8	NLTT 43806	1653+385	H	5,900	No	−7.1	9	Zuckerman et al. 2011
9	GD 362	1729+371	He	10,500	Yes	−5.98	16	Xu et al. 2013b, Zuckerman et al. 2007
10		1929+012	H	21,200	Yes	−4.10	12	Gaensicke et al. 2012, Vennes et al. 2011, Melis et al. 2011
11	G241-6	2222+683	He	15,300	No	−6.26	11	Jura et al. 2012, Xu et al. 2013b
12	HS 2253+8023	2253+803	He	14,400	No	−6.10	8	Klein et al. 2011
13	G29-38	2326+049	H	11,800	Yes	−5.77	8	Xu et al. 2014

[1]This table lists those white dwarfs where detections of Si, Mg, and Fe have been reported. Listed are the star number used in the figures and **Table 2**; two versions of the star's name; the dominant light element in the star's atmosphere (Dom.); the star's effective temperature (T_*); whether the star has an infrared excess from circumstellar dust; the logarithmic value of the Mg abundance by number relative to the dominant element, [Mg]/[X] = log n(Mg)/n(X); the number of elements heavier than helium that have been convincingly detected within the atmosphere; and relevant references. For WD 1929+012, where there is some disagreement about the true abundances, to be consistent with data for the other stars we heavily weight the results acquired at the Keck 10-m telescope by Melis et al. (2011).

calcium-aluminum-rich inclusions found in meteorites (Grossman 1980). These scenarios are not supported by current evidence (Jura & Xu 2013). As illustrated in **Figure 3**, the same four elements that dominate the composition of Earth also constitute more than 85% of the measured mass in extrasolar planetesimals in all systems where all four of these elements have been measured.

5.2. The Important Case of Carbon

Solid planetesimals are not simply accumulations of interstellar grains. If so, they would be at least 10% by mass composed of carbon, the most abundant heavy element after oxygen in the Sun (Lodders 2003). Instead, as first noted in Jura (2006) and as shown in **Figure 4** with much more data, this element is deficient by a factor of 10 or more both within the inner Solar System as represented by chondrites and among those extrasolar planetesimals that have been accreted onto white dwarfs.[1] The usual explanation for the lack of carbon within rocky material is that this element is volatile in an idealized nebular environment where all elements are initially gaseous (Lodders 2003). However, carbon has a complex chemistry, and rather than simply invoking

[1]In our figures we also show abundances in the photospheres for a local sample of F- and G-type main-sequence stars. There are relatively few spectral lines in A-type main-sequence stars, and these objects are therefore not as comprehensively analyzed.

Table 2 Measured abundances by number relative to Mg[1]

Number[2]	C	O	Mn	Cr	Si	Fe	Ni	Ca	Ti	Al
1 (He)	0.025	3.8	0.0036	0.0078	0.58	0.54	0.023	0.20	0.0039	0.071
2 (He)	<0.0039	5.5	—	<0.049	0.74	0.12	<0.077	0.078	<0.012	<0.078
3 (He)	—	7.4	0.0037	0.0083	0.60	0.50	0.023	0.028	0.00054	0.019
4 (H)	0.0050	1.0	—	0.16	0.63	2.5	0.050	—	—	0.032
5 (H)	<0.0020	0.63	—	—	0.079	0.63	—	0.071	—	—
6 (He)	0.50	—	0.0051	0.017	1.1	1.2	0.055	0.28	0.011	<0.46
7 (H)	0.0050	4.5	—	—	1.0	1.0	<0.050	0.18	—	0.28
8 (H)	—	—	—	0.0035	0.79	0.20	0.010	0.16	0.0035	0.32
9 (He)	0.19	<6.9	0.032	0.037	1.4	2.1	0.081	0.55	0.011	0.38
10 (H)	0.0020	1.0	0.0069	0.015	0.56	1.0	0.0025	0.019	—	0.0079
11 (He)	<0.0058	4.2	0.0032	0.0063	0.44	0.28	0.013	0.091	0.0019	<0.036
12 (He)	<0.01:	5.4	0.0051	0.013	0.68	0.89	0.06:	0.13	0.0024	<0.30
13 (H)	0.074	5.9	<0.037	0.018	1.5	0.74	<0.030	0.15	0.0074	<0.47
CI	0.74	7.3	0.0088	0.013	0.96	0.83	0.046	0.057	0.0023	0.080

[1]We list measured abundance ratios by number relative to Mg for the stars listed in Table 1 and for CI chondrites from Lodders (2003); error estimates are provided in the original references. These results are not corrected for settling times. Elements are arranged in order of volatility according to Lodders (2003). Colons denote values that are particularly uncertain.

[2]For convenience, the dominant constituent in the atmosphere is listed in parentheses after the star number.

thermodynamics, it may be more appropriate to consider detailed chemical-kinetic pathways in the protoplanetary disk that are powerful and efficient to explain carbon's absence in rocky materials (e.g., Lee et al. 2010).

There have been various observational and theoretical arguments for the existence of carbon-rich planets. These scenarios, which can be evaluated indirectly by studying externally polluted white dwarfs, are the following. (*a*) Although controversial (Fortney 2012, Nissen 2013), some stars may have sufficiently high carbon-to-oxygen ratios that nebular solids are largely carbonaceous and carbon-rich planetesimals ensue (Bond et al. 2010, Petigura & Marcy 2011). (*b*) Even if a disk has more oxygen than carbon, there may be a zone where the solids are largely carbonaceous (Lodders 2004). This putative zone would lie in between the snow line (where water sublimates) and a soot line (where carbon-rich particles sublimate). In this zone, carbon-rich planetesimals and ultimately carbon-rich planets might form. (*c*) It has been argued that the detection of CO in the atmospheres of warm extrasolar Jupiters indicates carbon-rich planets (Madhusudhan 2012). (*d*) It has been suggested that the mass-radius value for some extrasolar planets can be explained if they are carbon-rich (Madhusudhan et al. 2012). Overall, given the low carbon abundances in extrasolar rocky planetesimals, all four of these scenarios for the existence of carbon-rich planets need to be treated with caution.

5.3. The Lack of Water

Oxygen is so cosmically abundant that H_2O is predicted to be as much as 50% of the mass of solid planets that form in regions where the temperature in the planet-forming disk is sufficiently low that water ice is stable. Although water is abundant in the outer Solar System (Jewitt et al. 2007, Encrenaz 2008), the inner Solar System is comparatively dry; both bulk Earth and most meteorites are less than 1% water (Wasson & Kallemeyn 1988, Marty 2012). Models for snow

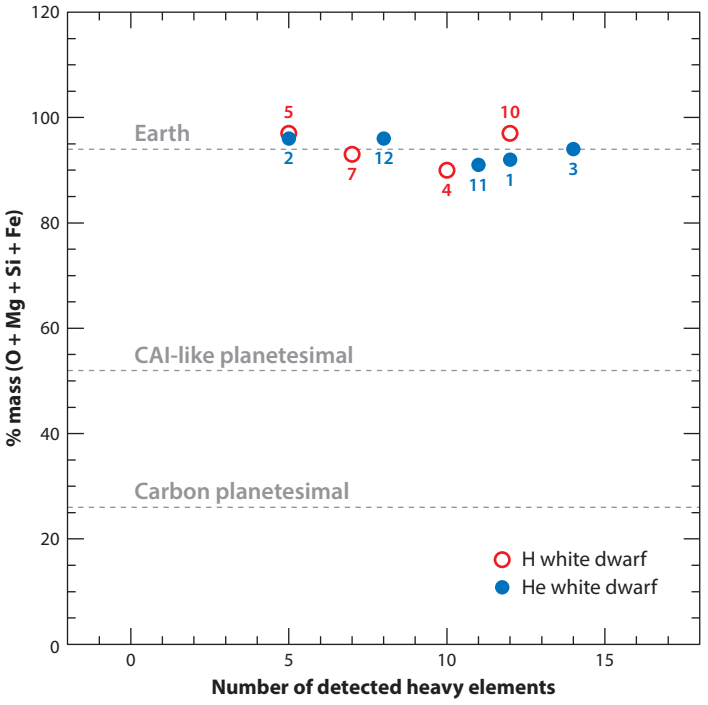

Figure 3

Percentage of mass within the four dominant elements for nine representative polluted white dwarfs where oxygen is confidently detected. Each point is labeled with its star number from **Table 1**; the dashed gray horizontal line at 94% represents the fraction of mass carried by these four elements in Earth. The other two dashed gray horizontal lines for putative extrasolar asteroids are taken from models of Bond et al. (2010). Objects largely composed of refractory elements are essentially very large versions of calcium-aluminum-rich inclusions (CAIs) and are predicted to possess detectable amounts of oxygen. Carbon-dominated planets are thought to possess a large amount of Si in the form of SiC. No exotic extrasolar planetesimals are currently known.

lines have been developed for protoplanetary disks to explain this dramatic contrast in water content (Lecar et al. 2006).

The water accreted by white dwarfs from extrasolar planetesimals is dissociated into oxygen and hydrogen; we cannot directly detect H_2O in the stellar photospheres.[2] Nevertheless, by examining the total fractions of these elements in the parent bodies, it is possible to constrain the amount of water they contain. Because the heat diffusion timescale is longer than the era of intense heating while its host star is luminous, water ice should survive within a planetesimal larger than 60 km in diameter even during a star's high-luminosity red giant phase before it evolves into a white dwarf (Jura & Xu 2010). Further, because extrasolar asteroids could contain hydrated minerals, we might detect substantial amounts of H and associated O in planetesimals accreted onto white dwarfs. However, currently, there is little evidence for much water. In the white dwarf with the most known accreted mass, WD J0738+1835, Dufour et al. (2012) found that there is so little H that the parent body was composed by mass of at most 1% water. For less highly polluted white dwarfs, a statistical approach can be adopted. In white dwarfs with helium-dominated atmospheres, hydrogen never

[2] H_2 has been detected in externally polluted white dwarfs (Xu et al. 2013a).

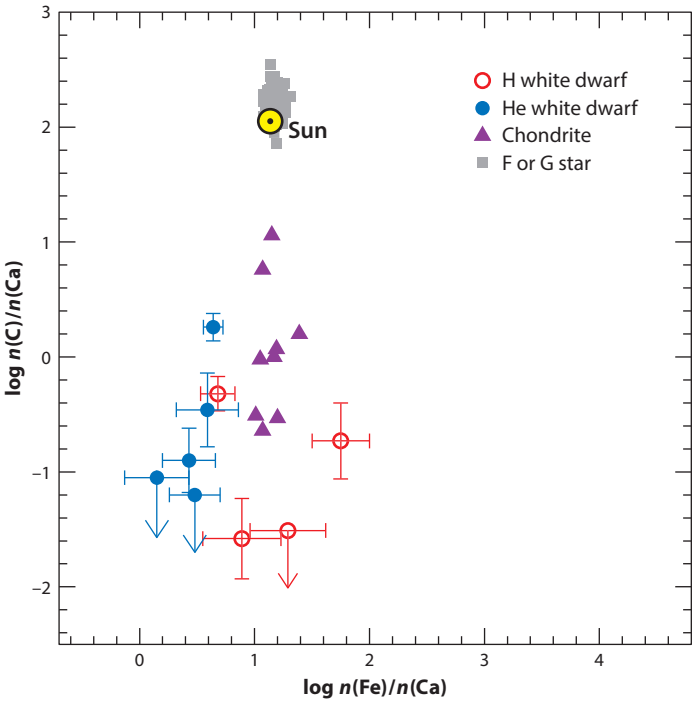

Figure 4

Logarithm of the relative numbers of Fe and C scaled to Ca for nine externally polluted white dwarfs listed in **Tables 1** and **2** (numbers 1, 2, 5, 6, 7, 9, 10, 11, 13). The purple triangles represent the values for different chondrites as reported by Wasson & Kallemeyn (1988). The value for the Sun is from Lodders (2003); results for 178 local F and G stars (*gray squares*) are from Reddy et al. (2003). The errors are from the model atmosphere and analysis; they do not reflect uncertainties due to the accretion phase. Here, as in all subsequent figures, we use Equations 4 and 5 to describe the assumed parent body composition for the open and filled symbols, respectively. The carbon deficiency among extrasolar planetesimals is evident.

gravitationally settles, and the observed amount is accumulated over the entire cooling age of the star. There also might be a significant amount of primordial hydrogen that the white dwarf has retained from its formation (Bergeron et al. 2011). In contrast, oxygen gravitationally settles in a time typically less than or approximately equal to 1 Myr. However, for an entire ensemble of stars, we can compare the time-averaged hydrogen and oxygen accretion rates to bound the fraction of accreted water. Jura & Xu (2012) constructed a catalog of all 57 known DB white dwarfs within 80 pc of the Sun for which the mean cooling age is 230 Myr. They used available data to estimate that the summed H accretion rate onto all 57 stars was less than or equal to 1.4×10^7 g s^{-1}. If all of this accreted hydrogen is carried in water, then the implied upper limit to the accretion of oxygen in water is 1.1×10^8 g s^{-1}. Oxygen has been reported in only 5 of the 57 stars in this sample (Desharnais et al. 2008; Jura & Xu 2010; Klein et al. 2010, 2011; Farihi et al. 2011; Jura et al. 2012; Xu et al. 2013b). Nevertheless, based on the recently updated oxygen settling times (Koester 2013), among these 5 stars, the summed oxygen accretion rate is 2.4×10^9 g s^{-1}. Therefore, even if accretion onto the remaining 52 stars is neglected, no more than 5.8% of the oxygen that is accreted onto the local ensemble of stars could have been carried in water. Consequently, viewed as an ensemble, the parent bodies are relatively dry.

There may, of course, be individual exceptions. Farihi et al. (2011, 2013) have argued that there is so much O compared with Mg, Si, and Fe in the accretion onto GD 61 that perhaps 25% of

the parent body was composed of water. Another star that may have accreted from a water-rich parent body is GD 378 (Jura & Xu 2010).

All these arguments apply to white dwarfs warmer than 10,000 K, because it is only in these objects where oxygen has been detected. White dwarfs warmer than 10,000 K typically have been cooling since their initial white dwarf phase for less than 1 Gyr; lower-temperature white dwarfs are older. At least in simple models, ensembles of planetesimals are depopulated from the inside out. Therefore, on average, older white dwarfs may accrete a population of planetesimals that originate relatively far from the host star (Xu & Jura 2012). If so, and if they were created beyond the snow line, they may be ice-rich.

6. EVIDENCE FOR DIFFERENTIATION AND COLLISIONS: BEYOND-NEBULAR EVOLUTION

Studies of individual objects have suggested peculiar abundances that can be explained as a result of sampling a distinctive portion of a differentiated planetesimal. Zuckerman et al. (2011) have argued that NLTT 43806 has accreted an Al-rich, Fe-poor object that was remnant of a planetary crust. Melis et al. (2011) and Gaensicke et al. (2012) have argued that WD 1929+012 and PG 0843+516, respectively, are Fe-rich as expected for objects with an iron core that have been at least partially stripped of their outer mantle and crust. Farihi et al. (2011) have argued that GD 61 is Fe-poor because it was formed by a collision in which the Fe core was lost. Here, instead of focusing on individual objects, we consider the abundance patterns of the ensemble of studied parent bodies. With this approach, we can establish trends that are only hinted at by measurements of individual objects.

6.1. Fe and Siderophiles (Cr, Mn, Ni): Core Formation

We now consider the relative abundances of Fe and siderophile elements to assess whether core formation is important. We first show in **Figure 5** a plot of the observed ratios by number of Mn to Fe, n(Mn)/n(Fe), versus n(Cr)/n(Fe) for seven externally polluted white dwarfs, chondrites, and nearby F and G stars. We see that there is only a relatively small dispersion in n(Cr)/n(Fe), whereas n(Mn)/n(Fe) displays a somewhat larger range in both the polluted white dwarfs and the chondrites but not in the F and G stars. Because Mn has a condensation temperature near 1,100 K (Lodders 2003), it is modestly volatile in the context of the formation of the inner Solar System and therefore displays a greater range in chondritic compositions (see, for example, O'Neill & Palme 2008) than that displayed by more refractory elements such as Cr.

The abundance pattern of n(Ni)/n(Fe) versus n(Cr)/n(Fe) is displayed in **Figure 6**. Because Ni is a strong siderophile and more refractory than Mn, a closer correlation is expected between Fe and Ni than between Fe and Mn. Here, we see such tight clustering of the results for chondrites, local stars, and most polluted white dwarfs. The pattern of Ni/Cr/Fe among extrasolar planetesimals is similar to what is observed in the inner Solar System.

An important correlation for inferring the underlying physical processes that govern the compositions of the extrasolar planetesimals is shown in **Figure 7**, which displays n(Fe)/n(Si) versus n(Mg)/n(Si). It is apparent that the dispersion in n(Fe)/n(Si) is notably greater than the dispersion in n(Mg)/n(Si). A natural explanation for this difference in dispersion in both Solar System rocks and externally polluted white dwarfs is metal-silicate/oxide differentiation within rocky bodies. This is represented among Solar System objects by the range of n(Fe)/n(Si) spanned by estimates for bulk Mercury (large metal core) and bulk Moon (virtually no metal core). Consequently, the

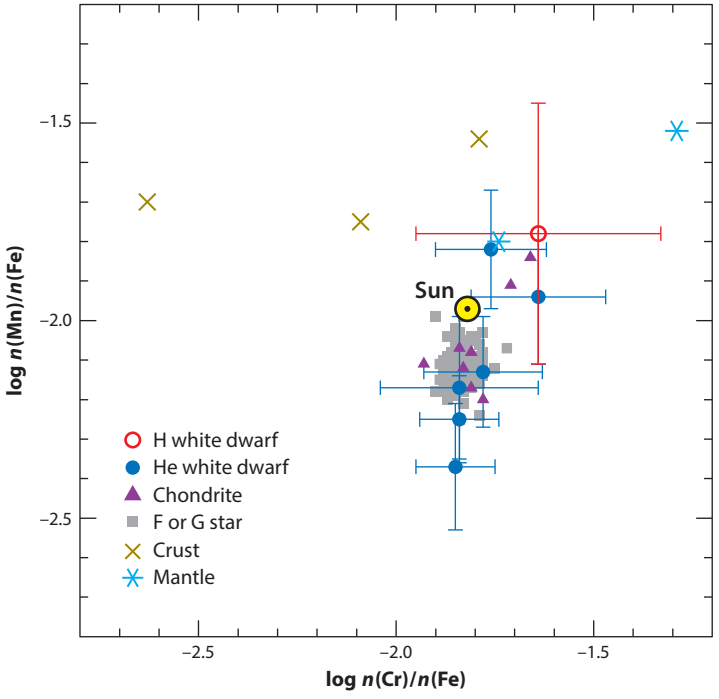

Figure 5

Plot of the relative abundance of Cr and Mn compared with Fe in seven externally polluted white dwarfs from **Table 1** (numbers 1, 3, 6, 9, 10, 11, 12) and, for comparison, local F- and G-type main-sequence stars and chondrites as described for **Figure 4**. Mantle rocks are represented by dunite in Earth (Hanghoj et al. 2010) and diogenite meteorites (Warren et al. 2009). Three crustal rocks are MORB (mid-ocean ridge basalt) (Presnall & Hoover 1987), eucrites (Warren et al. 2009), and the upper continental crust (Rudnick & Gao 2003).

data in **Figure 7** support the view that Fe cores have formed within a significant population of extrasolar planetesimals.

Consider two extreme cases plotted in **Figure 7**. The data for PG 1015+161 from Gaensicke et al. (2012) indicate a relatively low abundance of Si, leading to particularly high values of both n(Fe)/n(Si) and n(Mg)/n(Si). The Si abundance for this star is reported from UV data. Gaensicke et al. (2012) themselves note that there can be more than a factor of 3 disagreement between low-UV and high-optical determinations of the silicon abundance. In the case of this star, unpublished optical data from Keck (Xu et al. 2014) suggest that the Si abundance in this star may even be a factor of 10 greater than reported. Such extreme differences between the optical and UV results are rare and not understood. The extreme point displayed for PG 1015+161 must be treated with caution. Also shown in **Figure 7** is the point for GD 61 from Farihi et al. (2011), who argued that because the star has an infrared excess, the abundances in the photosphere can likely be described with a steady state. If so, they proposed that the Fe abundance is distinctly low because the white dwarf has only accreted the outer portion of a planetesimal that had an iron core. In this scenario, there is no reason to think that the Fe abundance is unusually low. Even if we exclude these two extreme points, the dispersion in n(Fe)/n(Si) is much greater than seen in chondrites or in the local F and G stars. It seems that Fe core formation is relatively common among extrasolar planetesimals.

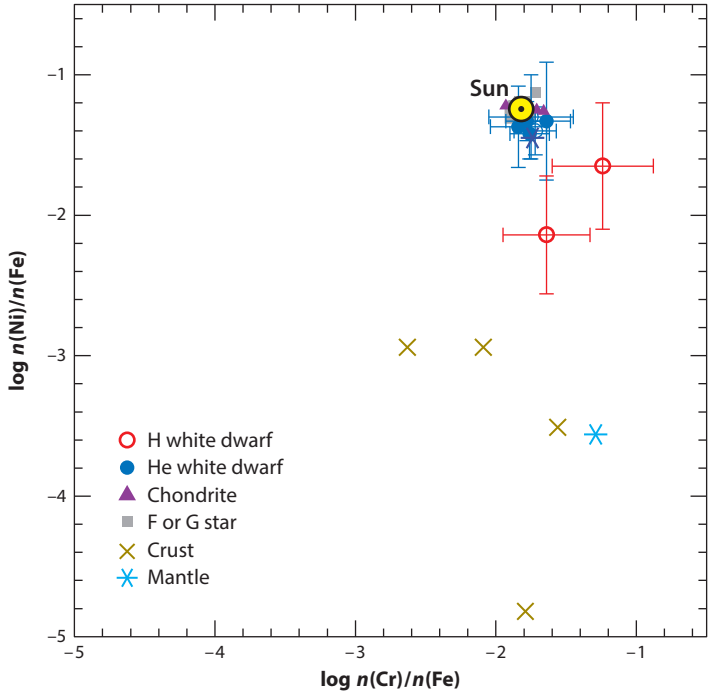

Figure 6

Plot of the relative abundance of Cr and Ni compared with Fe in eight externally polluted white dwarfs from **Table 1** (numbers 1, 3, 4, 6, 8, 9, 10, 11) and, for comparison, local F- and G-type main-sequence stars and chondrites as given in **Figure 4**. The mantle and crustal rocks are as described for **Figure 5**, as well as KREEP (potassium, rare earth elements, phosphorus) as an additional crustal rock (Taylor et al. 1991).

6.2. Refractory Lithophiles (Al, Ca, Ti): Crust Formation

If Fe-rich cores form, then there should also be Fe-poor crusts. In the Solar System, such crusts also are enriched in Al and Si. **Figure 8** displays the measurements of n(Si)/n(Al) versus n(Mg)/n(Al). For comparison, we also display the results for chondrites, local F and G stars, and both crustal and mantle rocks. Remarkably, the difference between crustal and mantle rocks is reflected in the range of compositions of extrasolar planetesimals. These data tend to confirm the suggestion that differentiation has occurred in a manner familiar from what is seen among Solar System objects.

There are puzzles in the complete suite of data for externally polluted white dwarfs. In **Figure 9**, we display n(Al)/n(Ca) versus n(Ti)/n(Ca). In chondrites and local stars, there is a small dispersion in the abundances ratios of these refractory elements. However, in the accreted parent bodies, there is a notably larger range. At the moment, we do not have any simple explanation for why the Ca fractional abundance tends to be high in some objects. It is notable that in a study of 26 lower-temperature white dwarfs with $T < 8{,}600$ K in which abundances of Mg, Ca, Fe, and Na were determined, the average value of n(Ca)/n(Mg) was in fact a factor of 1.4 lower than the solar value (Koester et al. 2011). Ca does not ubiquitously have an enhanced abundance within extrasolar planetesimals. Perhaps with more data to be plotted as in **Figure 9**, a pattern will emerge that will help explain this current mystery.

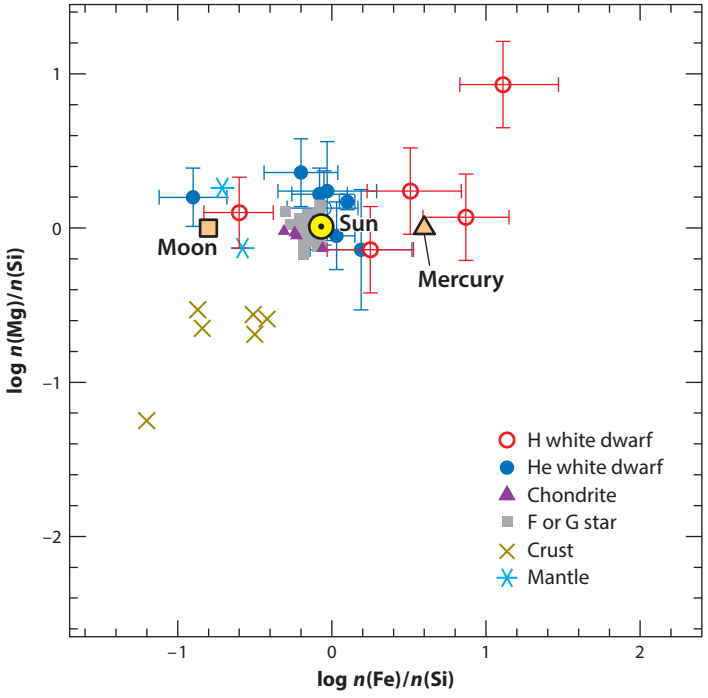

Figure 7

Plot of the relative abundance of Fe and Mg compared with Si in all thirteen externally polluted white dwarfs from **Table 1** and, for comparison, local F- and G-type main-sequence stars and chondrites as described for **Figure 4**. Besides the results for the crustal rocks displayed in **Figure 6**, we also include data for low-Ti and high-Ti lunar mare basalts (Taylor et al. 1991), bulk Moon (Warren 2005), and bulk Mercury (Brown & Elkins-Tanton 2009).

6.3. Collisional Blending

If planetesimals differentiate, then collisions may lead to the formation of objects with complex compositions by stripping mantles from cores. One such collision was important for the formation of the Moon (Canup 2004). More generally, the histories of Solar System meteorites (Goldstein et al. 2013, Scott et al. 2013) are explained by models invoking collisions among differentiated and stripped parent bodies.

We now consider externally polluted white dwarfs with particularly large numbers of detected heavy elements to assess whether models of collisions among differentiated objects explain the data. The best-studied case is the parent body accreted onto GD 362, which has 16 different individually detected elements (Xu et al. 2013b). Relative to CI chondrites, the material accreted onto GD 362 is deficient in volatiles such as C, Na, and Mn and enhanced in refractories such as Ca, Ti, Al, and Sr. However, the pattern is not simple. There is also a modest enhancement of Fe and a slight deficiency in Si. Using a χ^2 analysis to compare with a library of meteoritic compositions, Xu et al. (2013b) found that the composition of the material accreted onto GD 362 best resembles that of mesosiderites, although the match is not perfect. In standard models, mesosiderites are understood as the consequence of collisions that lead to blending between differentiated parent bodies (Scott et al. 2001).

The material accreted onto PG 1225-079 is another instance in which the composition of the parent body does not match any known Solar System meteorite (Xu et al. 2013b). A particular

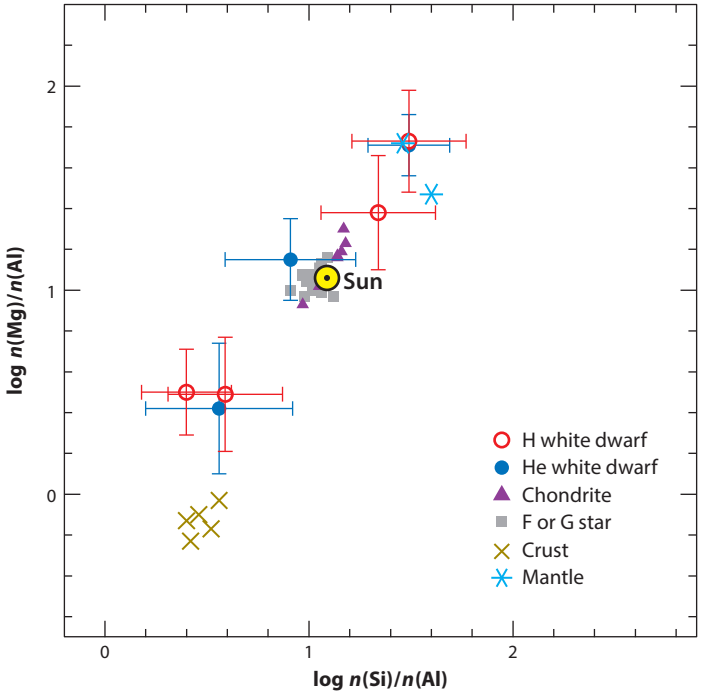

Figure 8

Plot of the relative abundance of Si and Mg compared with Al in seven externally polluted white dwarfs from **Table 1** (numbers 1, 3, 4, 7, 8, 9, 10) and, for comparison, local F- and G-type main-sequence stars, chondrites, and the same mantle and crustal rocks displayed in **Figure 7**.

puzzle is that carbon constitutes ~2% of the total accreted mass as also measured in CI chondrites. However, the upper limit to the mass fraction of sulfur accreted onto this star is 3×10^{-3}, whereas, in contrast, CI chondrites are approximately 6% composed of sulfur. Why is sulfur, which is less refractory than carbon, much more depleted in the parent body? There is no single Solar System counterpart. However, a collisional blend of a ureilite and mesosiderite material provides moderate agreement with the data (Xu et al. 2013b), again suggesting that collisions and differentiation are important processes among extrasolar planetesimals.

6.4. Model for Differentiation

Solar System asteroids are usually assumed to differentiate because soon after they are formed, they are heated by the decay of ^{26}Al, with a mean life of 1.03 Myr, to melt internally (Ghosh & McSween 1998). Because differentiation among extrasolar planetesimals appears widespread, Jura et al. (2013) have proposed that ^{26}Al is typically present in star-forming interstellar clouds with a concentration similar to that found within the young Solar System. If so, then contrary to many previous scenarios (Gritschneder et al. 2012), our Solar System was not unusual. Interstellar ^{26}Al appears largely concentrated into star-forming regions rather than being dispersed evenly throughout the entire Milky Way, consistent with evidence from measurements of gamma ray fluxes from the interstellar medium (Martin et al. 2009). [Note: There is a typographical error in Jura et al. (2013). The value for Q_0 employed in equation 5 of that paper should have been given as 1.2×10^{13} J kg^{-1}.]

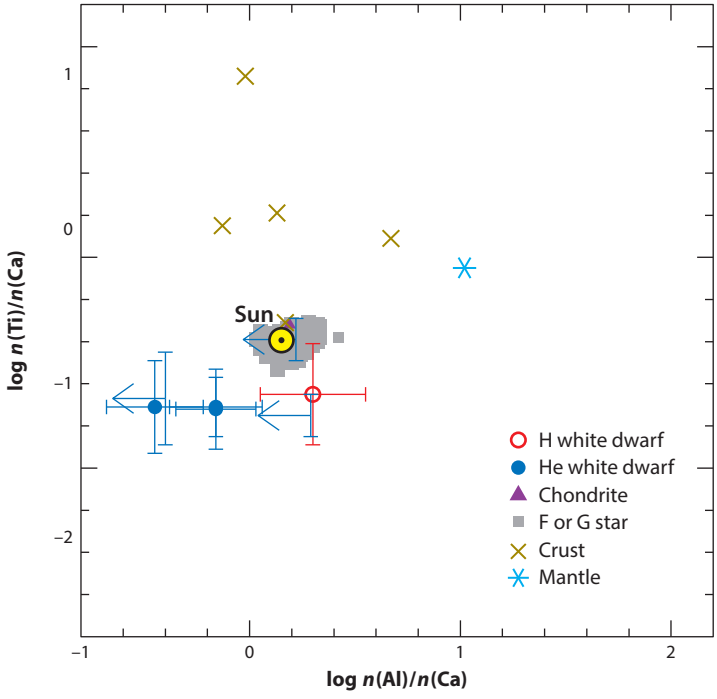

Figure 9

Plot of the relative abundance of Al and Ti compared with Ca in seven externally polluted white dwarfs listed in **Table 1** (numbers 1, 3, 6, 8, 9, 11, 12), and, for comparison, local F- and G-type main-sequence stars, chondrites, and the same mantle and crustal rocks displayed in **Figure 7**.

7. CONCLUSIONS AND FUTURE DIRECTIONS

Using externally polluted white dwarfs as a tool, we now have the capability to measure the elemental compositions of extrasolar planetesimals. First, as in bulk Earth, we find that O, Mg, Si, and Fe dominate, while C and water are trace constituents. There is good evidence that differentiation into Fe-rich cores and Al-rich crusts has occurred. A puzzle has arisen: In some instances, the amount of Ca is unexpectedly high.

We see three high-priority programs for the future. First, because there are fewer than a dozen white dwarfs with published measurements of eight or more detected elements, increasing the number of detailed studies of highly polluted stars is a high priority. Second, UV observations of polluted white dwarfs are extremely powerful for measuring the abundances of important volatile elements such as C and S. These studies should be continued. Third, looking for abundance patterns as a function of white dwarf mass and age may allow for reconstruction of the orbital architectures of extrasolar planetesimals; different populations may accrete onto different mass stars at different eras. Altogether, these observational programs will enable a much deeper understanding of the physical processes that control the formation and evolution of extrasolar rocky planets.

DISCLOSURE STATEMENT

The authors are not aware of any affiliations, memberships, funding, or financial holdings that might be perceived as affecting the objectivity of this review.

ACKNOWLEDGMENTS

This work has been partly supported by NASA and the National Science Foundation.

LITERATURE CITED

Aannestad PA, Kenyon SJ, Hammond GL, Sion EM. 1993. Cool metallic-line white dwarfs, radial velocities, and interstellar accretion. *Astron. J.* 105:1033–44

Absil O, Defrere D, Coude du Foresto V, Di Folco E, Merand A, et al. 2013. A near-infrared interferometric survey of debris-disc stars. III. First statistics based on 42 stars observed with CHARA/FLUOR. *Astron. Astrophys.* 555:104A

Alcock C, Fristrom CC, Siegelman R. 1986. On the number of comets around other single stars. *Astrophys. J.* 302:462–76

Barber SD, Patterson AJ, Kilic M, Leggett SK, Dufour P, et al. 2012. The frequency of debris disks at white dwarfs. *Astrophys. J.* 760:26

Becklin EE, Farihi J, Jura M, Song I, Weinberger A, et al. 2005. A dusty disk around GD 362, a white dwarf with a uniquely high photospheric metal abundance. *Astrophys. J. Lett.* 632:L119–22

Bergeron P, Wesemael F, Dufour P, Beauchamp A, Hunter C, et al. 2011. A comprehensive spectroscopic analysis of DB white dwarfs. *Astrophys. J.* 737:28

Bond JC, O'Brien DP, Lauretta DS. 2010. The compositional diversity of extrasolar terrestrial planets. I. In situ simulations. *Astrophys. J.* 715:1050–70

Bonsor A, Mustill AJ, Wyatt MC. 2011. Dynamical effects of stellar mass-loss on a Kuiper-like belt. *MNRAS* 414:930–39

Brown SM, Elkins-Tanton LT. 2009. Compositions of Mercury's earliest crust from magma ocean models. *Earth Planet. Sci. Lett.* 286:446–55

Canup RM. 2004. Dynamics of lunar formation. *Annu. Rev. Astron. Astrophys.* 42:441–75

Chayer P, Fontaine G, Wesemael F. 1995. Radiative levitation in hot white dwarfs: equilibrium theory. *Astrophys. J. Suppl.* 99:189–221

Chen CH, Jura M. 2001. A possible massive asteroid belt around ζ Leporis. *Astrophys. J. Lett.* 560:L171–74

Chen CH, Sargent BA, Bohac C, Kim KH, Leibensperger E, et al. 2006. Spitzer IRS spectroscopy of IRAS-discovered debris disks. *Astrophys. J. Suppl.* 166:351–77

Davidsson BJR. 1999. Tidal splitting and rotational breakup of solid spheres. *Icarus* 142:525–35

Debes JH, Sigurdsson S. 2002. Are there unstable planetary systems around white dwarfs? *Astrophys. J.* 572:556–65

Debes JH, Kilic M, Faedi, F, Shkolnik EL, Lopez-Morales M, et al. 2012a. Detection of weak circumstellar gas around the DAZ white dwarf WD 1124−293: evidence for the accretion of multiple asteroids. *Astrophys. J.* 754:59

Debes JH, Walsh KJ, Stark C. 2012b. The link between planetary systems, dusty white dwarfs, and metal-polluted white dwarfs. *Astrophys. J.* 747:148

Desharnais S, Wesemael F, Chayer P, Kruk JW, Saffer RA. 2008. *FUSE* observations of heavy elements in the photospheres of cool DB white dwarfs. *Astrophys. J.* 672:540–52

Dickinson NJ, Barstow MA, Welsh BY, Burleigh M, Farihi J, et al. 2012. The origin of hot white dwarf circumstellar features. *MNRAS* 423:1397–410

Dufour P, Bergeron P, Liebert J, Harris HC, Knapp GR, et al. 2007. On the spectral evolution of cool, helium-atmosphere white dwarfs: detailed spectroscopic and photometric analysis of DZ stars. *Astrophys. J.* 663:1291–308

Dufour P, Kilic M, Fontaine G, Bergeron, P, Melis C, et al. 2012. Detailed compositional analysis of the heavily polluted DBZ white dwarf SDSS J073842.56+183509.06: a window on planet formation? *Astrophys. J.* 749:6

Duncan MJ, Lissauer JJ. 1998. The effects of post-main-sequence solar mass loss on the stability of our planetary system. *Icarus* 134:303–10

Dupuis J, Fontaine G, Pelletier C, Wesemael F. 1992. A study of metal abundance patterns in cool white dwarfs. I. Time-dependent calculations of gravitational settling. *Astrophys. J. Suppl.* 82:505–21

Dupuis J, Fontaine G, Wesemael F. 1993. A study of metal abundance patterns in cool white dwarfs. III. Comparison of the predictions of the two-phase accretion model with the observations. *Astrophys. J. Suppl.* 87:345–65

Encrenaz T. 2008. Water in the Solar System. *Annu. Rev. Astron. Astrophys.* 46:57–87

Farihi J, Brinkworth CS, Gaensicke BT, Marsh TR, Girven J, et al. 2011. Possible signs of water and differentiation in a rocky exoplanetary body. *Astrophys. J. Lett.* 728:L8

Farihi J, Gaensicke BT, Koester D. 2013. Evidence for water in the rocky debris of a disrupted extrasolar minor planet. *Science* 342:218–20

Farihi J, Gaensicke BT, Steele PR, Girven J, Burleigh MR, et al. 2012a. A trio of metal-rich dust and gas discs found orbiting candidate white dwarfs with *K*-band excess. *MNRAS* 421:1635–43

Farihi J, Gaensicke BT, Wyatt MC, Girven J, Pringle JE, et al. 2012b. Scars of intense accretion episodes at metal-rich white dwarfs. *MNRAS* 424:464–71

Farihi J, Jura M, Zuckerman B. 2009. Infrared signatures of disrupted minor planets at white dwarfs. *Astrophys. J.* 694:805–19

Fortney JJ. 2012. On the carbon-to-oxygen ratio measurement in nearby Sun-like stars: implications for planet formation and the determination of stellar abundances. *Astrophys. J. Lett.* 747:L27

Gaensicke BT, Koester D, Farihi J, Girven J, Parsons SG, et al. 2012. The chemical diversity of exo-terrestrial planetary debris around white dwarfs. *MNRAS* 424:333–47

Gaensicke BT, Koester D, Marsh TR, Rebassa-Mansergas A, Southworth J. 2008. SDSS J084539.17+225728.0: the first DBZ white dwarf with a metal-rich gaseous debris disc. *MNRAS Lett.* 391:L103–7

Gaensicke BT, Marsh TR, Southworth J. 2007. SDSS J104341.53+085558.2: a second white dwarf with a gaseous debris disc. *MNRAS Lett.* 380:L35–39

Gaensicke BT, Marsh TR, Southworth J, Rebassa-Mansergas A. 2006. A gaseous metal disk around a white dwarf. *Science* 314:1908–10

Ghosh A, McSween HY. 1998. A thermal model for the differentiation of asteroid 4 Vesta, based on radiogenic heating. *Icarus* 134:187–206

Gianninas A, Dufour P, Bergeron P. 2004. Discovery of a cool, massive, and metal-rich DAZ white dwarf. *Astrophys. J. Lett.* 617:L57–60

Girven J, Brinkworth CS, Farihi J, Gaensicke BT, Hoard DW et al. 2012. Constraints on the lifetimes of disks resulting from tidally destroyed rocky planetary bodies. *Astrophys. J.* 749:154

Goldstein JI, Scott ERD, Winfield T, Yang J. 2013. Thermal histories of group IAB and related iron meteorites and comparison with other groups of irons and stony iron meteorites. *Lunar Planet. Sci. Conf. Abstr.* 44:1394

Gritschneder M, Lin DNC, Murray SD, Yin Q-Z, Gong M-N. 2012. The supernova triggered formation and evolution of the Solar System. *Astrophys. J.* 745:22

Grossman L. 1980. Refractory inclusions in the Allende meteorite. *Annu. Rev. Earth Planet. Sci.* 8:559–608

Hanghoj K, Kelemen PB, Hassler D, Godard M. 2010. Composition and genesis of depleted mantle peridotites from the Wadi Tayin Massif, Oman Ophiolite; major and trace element geochemistry, and Os isotope and PGE systematics. *J. Petrol.* 51:201–27

Hansen BMS, Liebert J. 2003. Cool white dwarfs. *Annu. Rev. Astron. Astrophys.* 41:465–515

Jewitt D, Chizmadia L, Grimm R, Prialnik D. 2007. Water in the small bodies of the Solar System. In *Protostars and Planets*, Vol. 5, ed. B Reipurth, D Jewitt, K Keil, pp. 863–78. Tucson: Univ. Ariz. Press

Jura M. 2003. A tidally disrupted asteroid around the white dwarf G29-38. *Astrophys. J. Lett.* 584:L91–94

Jura M. 2006. Carbon deficiency in externally polluted white dwarfs: evidence for accretion of asteroids. *Astrophys. J.* 653:613–20

Jura M. 2008. Pollution of single white dwarfs by accretion of many small asteroids. *Astron. J.* 135:1785–92

Jura M. 2014. The elemental compositions of extrasolar planetesimals. In *Formation, Detection and Characterization of Extrasolar Habitable Planets*, ed. N Haghighipour, J-L Zhou, pp. 100–9. IAU Symp. Proc. 293. Paris: IAU

Jura M, Farihi J, Zuckerman B. 2007. Externally polluted white dwarfs with dust disks. *Astrophys. J.* 663:1285–90

Jura M, Muno M, Farihi J, Zuckerman B. 2009. X-ray and infrared observations of two externally polluted white dwarfs. *Astrophys. J.* 699:1743–49

Jura M, Xu S. 2010. The survival of water within extrasolar minor planets. *Astron. J.* 140:1129–36

Jura M, Xu S. 2012. Water fractions in extrasolar planetesimals. *Astron. J.* 143:6

Jura M, Xu S. 2013. Extrasolar refractory-dominated planetesimals: an assessment. *Astron. J.* 145:30

Jura M, Xu S, Klein B, Koester D, Zuckerman B. 2012. Two extrasolar asteroids with low volatile-element mass fractions. *Astrophys. J.* 750:69

Jura M, Xu S, Young ED. 2013. ^{26}Al in the early Solar System: not so unusual after all. *Astrophys. J. Lett.* 775:L41

Kawka A, Vennes S, Dinnbier F, Cibulkova H, Nemeth P. 2011. Abundance analysis of DAZ white dwarfs. *Planetary Systems Beyond the Main Sequence*, ed. S Schuh, H Drechsel, U Heber, pp. 238–45. AIP Conf. Proc. 1331. Melville, NY: AIP

Kilic M, von Hippel T, Leggett S, Winget DE. 2005. Excess infrared radiation from the massive DAZ white dwarf GD 362: a debris disk? *Astrophys. J. Lett.* 632:L115–18

Kilic M, von Hippel T, Leggett S, Winget DE. 2006. Debris disks around white dwarfs: the DAZ connection. *Astrophys. J. Lett.* 646:474–79

Klein B, Jura M, Koester D, Zuckerman B. 2011. Rocky extrasolar planetary compositions derived from externally polluted white dwarfs. *Astrophys. J.* 741:64

Klein B, Jura M, Koester D, Zuckerman B, Melis C. 2010. Chemical abundances in the externally polluted white dwarf GD 40: evidence of a rocky extrasolar minor planet. *Astrophys. J.* 709:950–62

Kleinman SJ, Kepler SO, Koester D, Pelisoli I, Pecanha V, et al. 2013. SDSS DR7 white dwarf catalog. *Astrophys. J. Suppl.* 204:5

Koester D. 2009. Accretion and diffusion in white dwarfs. New diffusion timescales and applications to GD 362 and G 29-38. *Astron. Astrophys.* 498:517–25

Koester D. 2013. *A cautionary note on diffusion timescales for white dwarfs*. Inst. Theor. Phys. Astrophys., Univ. Kiel, Ger., updated Jan. **http://www1.astrophysik.uni-kiel.de/~koester/astrophysics/**

Koester D, Gaensicke B, Girven J, Farihi J. 2013. Search for metal pollution in 81 DA white dwarfs. In *18th European White Dwarf Workshop*, ed. J Krzesinski, G Stachowski, P Moskalik, K Bajan, pp. 445–50. Astron. Soc. Pac. Conf. Ser. 469. Orem, UT: Astron. Soc. Pac.

Koester D, Girven J, Gaensicke BT, Dufour P. 2011. Cool DZ white dwarfs in the SDSS. *Astron. Astrophys.* 530:A114

Koester D, Rollenhagen K, Napiwotzki R, Voss B, Christlieb N, et al. 2005. Metal traces in white dwarfs of the SPY (ESO Supernova Ia Progenitor Survey) sample. *Astron. Astrophys.* 432:1025–32

Koester D, Wilken D. 2006. The accretion-diffusion scenario for metals in cool white dwarfs. *Astron. Astrophys.* 453:1051–57

Krasinsky GA, Petjeva EV, Vasilyev MV, Yagudina EI. 2002. Hidden mass in the asteroid belt. *Icarus* 158:98–105

Lecar M, Podolak M, Sasselov D, Chiang E. 2006. On the location of the snow line in a protoplanetary disk. *Astrophys. J.* 640:1115–18

Lee J-E, Bergin EA, Nomura H. 2010. The solar nebula on fire: a solution to the carbon deficit in the inner Solar System. *Astrophys. J. Lett.* 710:L21–25

Lodders K. 2003. Solar System abundances and condensation temperatures of the elements. *Astrophys. J.* 591:1220–47

Lodders K. 2004. Jupiter formed with more tar than ice. *Astrophys. J.* 611:587–97

Madhusudhan N. 2012. C/O ratio as a dimension for characterizing exoplanetary atmospheres. *Astrophys. J.* 758:36

Madhusudhan N, Lee KKM, Mousis O. 2012. A possible carbon-rich interior in super-Earth 55 Cancri e. *Astrophys. J. Lett.* 759:L40

Martin P, Knoedlseder J, Diehl R, Meynet G. 2009. New estimates of the gamma-ray line emission of the Cygnus region from INTEGRAL/SPI observations. *Astron. Astrophys.* 506:703–10

Marty B. 2012. The origins and concentrations of water, carbon, nitrogen and noble gases on Earth. *Earth Planet. Sci. Lett.* 313:56–66

McCook GP, Sion EM. 1999. A catalog of spectroscopically identified white dwarfs. *Astrophys. J. Suppl.* 121:1–130

Melis C, Dufour P, Farihi J, Bochanski J, Burgassser AJ, et al. 2012. Gaseous material orbiting the polluted, dusty white dwarf HE 1349−2305. *Astrophys. J. Lett.* 751:L4

Melis C, Farihi J, Dufour P, Zuckerman B, Burgasser AJ, et al. 2011. Accretion of a terrestrial-like minor planet by a white dwarf. *Astrophys. J.* 732:90

Melis C, Jura M, Albert L, Klein B, Zuckerman B. 2010. Echoes of a decaying planetary system: the gaseous and dusty disks surrounding three white dwarfs. *Astrophys. J.* 722:1078–91

Metzger BD, Rafikov RR, Bochkarev KV. 2012. Global models of runaway accretion in white dwarf debris discs. *MNRAS* 423:505–28

Morales FY, Rieke GH, Werner MW, Bryden G, Stapelfeldt KR, et al. 2011. Common warm dust temperatures around main-sequence stars. *Astrophys. J.* 730:L29

Morales FY, Werner MW, Bryden G, Plavchan P, Stapelfeldt KR, et al. 2009. Spitzer mid-IR spectra of dust debris around A and late B type stars: asteroid belt analogs and power-law dust distributions. *Astrophys. J.* 699:1067–86

Nissen PE. 2013. The carbon-to-oxygen ratio in stars with planets. *Astron. Astrophys.* 552:A73

O'Neill HSC, Palme H. 2008. Collisional erosion and the non-chondritic composition of the terrestrial planets. *Philos. Trans. R. Soc. A* 366:4205-38

Petigura EA, Marcy GW. 2011. Carbon and oxygen in nearby stars: keys to protoplanetary disk chemistry. *Astrophys. J.* 735:41

Presnall DC, Hoover JD. 1987. High pressure phase equilibrium constraints on the origin of mid-ocean ridge basalts. In *Magmatic Processes: Physicochemical Principles*, ed. BO Mysen, pp. 75–89. Geochem. Soc. Spec. Publ. 1. Saint Louis, MO: Geochem. Soc.

Rafikov RR. 2011a. Metal accretion onto white dwarfs caused by Poynting–Robertson drag on their debris disks. *Astrophys. J. Lett.* 732:L3

Rafikov RR. 2011b. Runaway accretion of metals from compact discs of debris on to white dwarfs. *MNRAS Lett.* 416:L55–59

Reach WT, Kuchner, MJ, von Hippel T, Burrows A, Mullally F, et al. 2005. The dust cloud around the white dwarf G29-38. *Astrophys J. Lett.* 635:L161–64

Reddy BE, Tomkin J, Lambert DL, Prieto Allende C. 2003. The chemical compositions of galactic disk F and G dwarfs. *MNRAS* 340:304–40

Rudnick RL, Gao S. 2003. Composition of the continental crust. *Treatise Geochem.* 3:1–64

Scott ERD, Haack H, Love SG. 2001. Formation of mesosiderites by fragmentation and reaccretion of a large differentiated asteroid. *Meteorit. Planet. Sci.* 36:869–91

Scott ERD, Krot TV, Goldstein JI. 2013. Thermal and impact histories of ordinary chondrites and their parent bodies: constraints from metallic Fe-Ni in type 3 chondrites. *Lunar Planet. Sci. Conf. Abstr.* 44:1826

Sion EM, Kenyon SJ, Aannestad PA. 1990. An atlas of optical spectra of DZ white dwarfs and related objects. *Astrophys. J. Suppl.* 72:707–14

Su KYL, Rieke GH, Stansberry JA, Bryden G, Stapelfeldt KR, et al. 2006. Debris disk evolution around A stars. *Astrophys. J.* 653:675–89

Taylor JG, Warren P, Ryder G, Dalano J, Pieters C, et al. 1991. Lunar rocks. In *Lunar Sourcebook: A User's Guide to the Moon*, ed. GH Heiken, DT Vaniman, BM French, J Schmitt, pp. 183–284. Cambridge, UK: Cambridge Univ. Press

Vennes S, Kawka A, Nemeth P. 2011. Pressure shifts and abundance gradients in the atmosphere of the DAZ white dwarf GALEX J193156.8+011745. *MNRAS* 413:2545–53

Veras D, Mustill AJ, Bonsor A, Wyatt MC. 2013. Simulations of two-planet systems through all phases of stellar evolution: implications for the instability boundary and white dwarf pollution. *MNRAS* 431:1686–708

Veras D, Wyatt MC, Mustill AJ, Bonsor A, Eldridge JJ. 2011. The great escape: how exoplanets and smaller bodies desert dying stars. *MNRAS* 417:2104–23

Warren PH. 2005. "New" lunar meteorites: implications for composition of the global lunar surface, lunar crust, and the bulk Moon. *Meteorit. Planet. Sci.* 40:477–506

Warren PH, Kallemeyn GW, Huber H, Ulff-Moller F, Choe W. 2009. Siderophile and other geochemical constraints on mixing relationships among HED-meteoritic breccias. *Geochim. Cosmochim. Acta* 73:5918–43

Wasson JT, Kallemeyn GW. 1988. Compositions of chondrites. *Philos. Trans. R. Soc. A* 325:535–44

Williams KA, Bolte M, Koester D. 2009. Probing the lower mass limit for supernova progenitors and the high-mass end of the initial-final mass relation from white dwarfs in the open cluster M 35 (NGC 2168). *Astrophys. J.* 693:355–69

Xu S, Jura M. 2012. Spitzer observations of white dwarfs; the missing planetary debris around DZ stars. *Astrophys. J.* 745:88

Xu S, Jura M, Klein B, Koester D, Zuckerman B. 2013b. Two beyond-primitive extrasolar planetesimals. *Astrophys. J.* 766:132

Xu S, Jura M, Koester D, Klein B, Zuckerman B. 2013a. Discovery of molecular hydrogen in white dwarf atmospheres. *Astrophys. J. Lett.* 766:L18

Xu S, Jura M, Koester D, Klein B, Zuckerman B. 2014. Elemental compositions of two extrasolar rocky planetesimals. *Astrophys. J.* 783:79

Zuckerman B, Becklin EE 1987. Excess infrared radiation from a white dwarf—an orbiting brown dwarf? *Nature* 330:138–40

Zuckerman B, Koester D, Dufour P, Melis C, Klein B et al. 2011. An aluminum/calcium-rich, iron-poor, white dwarf star: evidence for an extrasolar planetary lithosphere? *Astrophys. J.* 739:101

Zuckerman B, Koester D, Melis C, Hansen B, Jura M. 2007. The chemical composition of an extrasolar minor planet. *Astrophys. J.* 671:872–77

Zuckerman B, Koester D, Reid IN, Hunsch M. 2003. Metal lines in DA white dwarfs. *Astrophys. J.* 596:477–95

Zuckerman B, Melis C, Klein B, Koester D, Jura M. 2010. Ancient planetary systems are orbiting a large fraction of white dwarf stars. *Astrophys. J.* 722:725–36

Annual Review
of Earth and
Planetary Sciences
Volume 42, 2014

Contents

Indexes

Errata

An online log of corrections to *Annual Review of Earth and Planetary Sciences* articles may be found at http://www.annualreviews.org/errata/earth